

Velocity analysis using prestack migration : Applications

Kamal Al-Yahya and Francis Muir

ABSTRACT

In a previous SEP report (SEP-38), Al-Yahya and Muir discussed employing prestack migration as a means of velocity estimation. This is a follow-up to that paper. We will continue the discussion of the subject and demonstrate its use. These examples show that migrated common receiver gathers are well-suited for velocity analysis.

INTRODUCTION

Jacobs (1982) proposed that profiles be migrated independently so that the aliasing of the shot axis is minimized. Another advantage of profile migration is that sampling of the geophone axis is better than that of the common midpoint axis (as long as the ratio of the shot interval to the receiver interval is greater than 1, which is the common goal and practice of seismic exploration). The improved sampling has the effect of reducing spatial aliasing, though we should remember to keep the receiver spacing small enough, especially when adverse conditions, such as steeply dipping reflectors, are present.

Al-Yahya and Muir (1984) suggested applying this technique to velocity estimation. Since our first report on this subject (in SEP-38; hereafter called Paper I), we have succeeded in obtaining more results. Some of these results were shown at the last SEP meeting (May 1984). In this paper we will show our current understanding of this subject and support it by examples. Also, after migrating with an initial velocity, we will attempt to quantify the error in the velocity function in our first trial

Yilmaz and Chambers (1984) used a scheme akin to the one that we use. However, their process begins with data in the (y, h) space, and then they do the migration in the Fourier domain. It is well known that working in the Fourier domain is not suited for media with lateral velocity variations. Another difference between the two methods relates to the velocity determination procedure. They made the velocity determination by looking at the output in the (t, τ) space, where t is the travel time and τ is the time-equivalent depth, to see if events fall along the line $t = \tau$. They mention that employing downward continuation to determine the medium's velocity is based on the principle, pointed out by Doherty and Cl erbout (1974), that downward continuing with the wrong velocity to the correct depth is equivalent to downward continuing with the correct velocity to the wrong depth.

Recording geometry

It is sometimes argued that profiles migration does not produce satisfactory results because of the poor coverage of profile recording. For this reason, we will digress here to discuss the importance of the recording geometry. Figure 1 shows the model that will be used in one of the later examples. It consists of a plane reflector dipping at an angle $\alpha = 30^\circ$. The medium has a constant velocity of 400 m/sec. The figure also shows a synthetic profile as recorded by a split-spread cable, and the result of migrating the synthetic profile using the correct velocity.

The point made here is that the satisfactory result of our migration is due to our use of a split-spread cable that received energy from within the lateral extent of the cable; this also means that we did not have to pad the data with zeros. Using an off-end shooting geometry, we could get either the left or the right side of the profile in Figure 1. If we had the left side, we would still expect to get a reasonable image, because most of the energy in the profile comes from the left. But if we recorded only the right side, the resulting image would not be correct, as shown in Figure 2. The usual solution to this problem is to pad the profile with zeros at the left; the extra space acts as a place for the energy to escape to. The result of this padding is shown in Figure 3, which shows an image still inferior to that of Figure 1. Of course we might have to do some padding even when we use split-spread recording, for example when we have steep and shallow reflectors. It should be observed however that using a wide-aperture recording (i.e., long cable) provides a better solution than padding.

DOING THE MIGRATION

In Paper I, we outlined a hybrid method in which we did the migration by downward

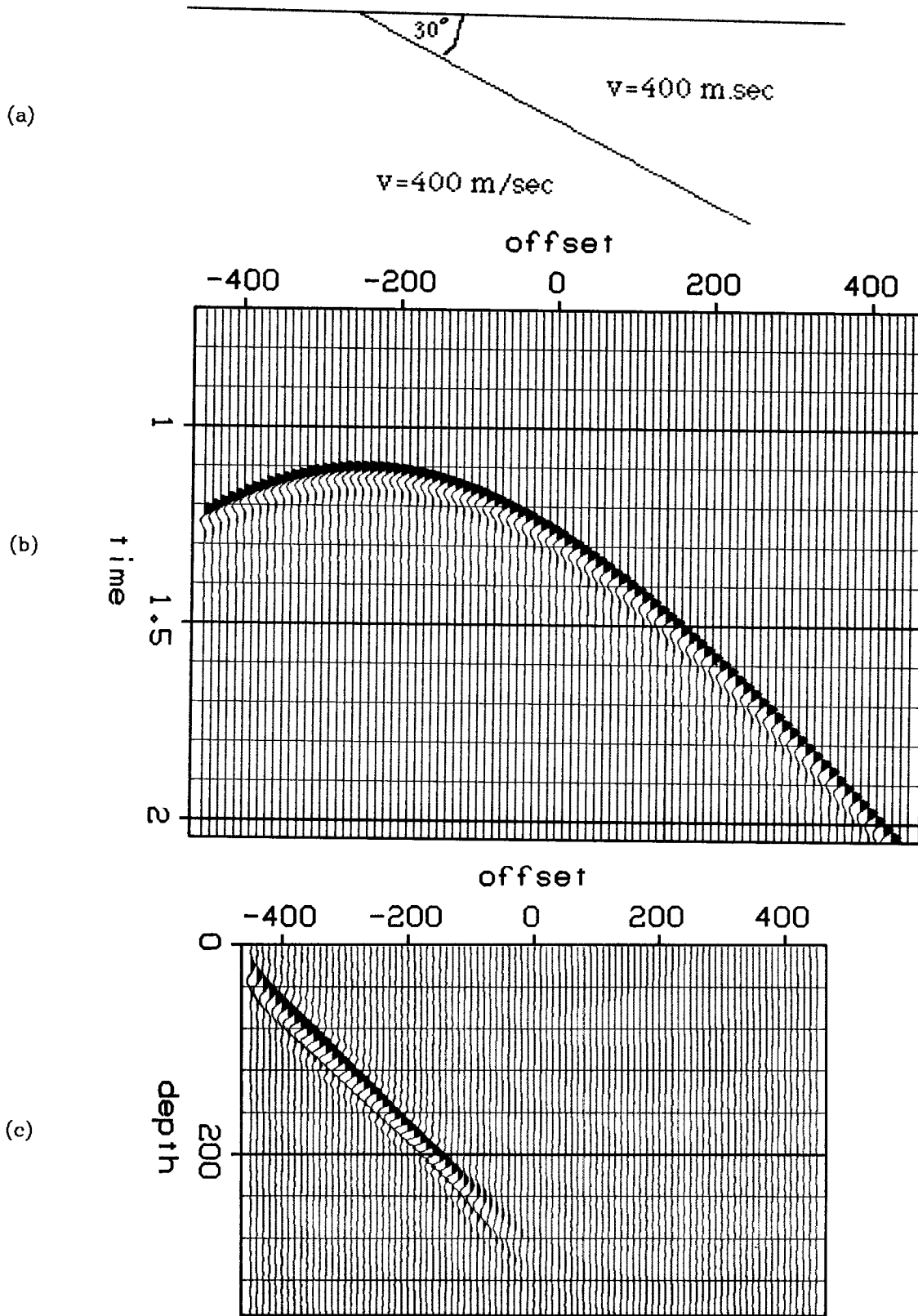


FIG. 1. (a) The model. (b) Primary-only split-spread synthetic profile from the model ($nt=1024$, $nx=91$, $dt=2$ msec, and $dx=10$ m.) (c) The migrated profile, $dz=6$ m.

continuing the receivers to a given level and then applying to each receiver, a time shift equal to the travel time between the source and the receiver. This travel time was calculated by raytracing, based upon our current velocity model. The example shown in Paper I and most of the examples here were derived by using this method. Ivan Psencik of the Czechoslovakian Academy of Science (private communication) has kindly provided us with a raytracing package. This raytracing package is fast for modeling work, but is too slow, especially if the model is complicated, for our purpose because many travel times must be calculated.

An alternative way is to downward continue both the source and the receivers to a specific depth and then use the imaging principle

$$R(x, z) = \sum_{\omega} \frac{U(x, z, \omega)}{D(x, z, \omega)} \quad ,$$

where $U(x, z, \omega)$ is the upgoing energy, $D(x, z, \omega)$ is the downgoing energy and $R(x, z)$ is the reflectivity (Jacobs 1982). There is a computational problem associated with this formula: the vanishing of $D(x, z, \omega)$ for some frequencies. For this reason, the formula is modified. A possible form is

$$R(x, z) = \frac{\sum_{\omega} U(x, z, \omega)D^*(x, z, \omega)}{\sum_{\omega} D(x, z, \omega)D^*(x, z, \omega) + \epsilon(x, z, \omega)} \quad ,$$

where $\epsilon(x, z, \omega)$ is added for stability. A suggested value for ϵ is $\sqrt{\max(DD^*)}$.

Kjartansson (1983) used the simplified form

$$R(x, z) = \sum_{\omega} U(x, z, \omega)D^*(x, z, \omega) \quad , \quad (1)$$

in which the downgoing field is correlated with the upgoing field.

Kjartansson kindly provided us his program that implements equation (1).

Figure 4 shows the model that we used for this type of prestack migration. We used raytracing to generate 100 split-spread field records, having 99 receivers each. We made the shot interval 40 m, the receiver interval 20 m, and the sampling interval 4 msec.

Some of these records are shown in Figure 5. We notice that in the synthetic data, there are shadow zones due to the sharp corners that exist in the model. These shadow zones do not of course exist in real data, because what travel in the earth are waves and not rays, and waves will reach everywhere. WE migrated the profiles using an arbitrary constant velocity of 2500 m/sec. Some of the migrated profiles are shown in Figure 6, and some migrated common receiver gathers (CRG's) are shown in Figure 7. We see that

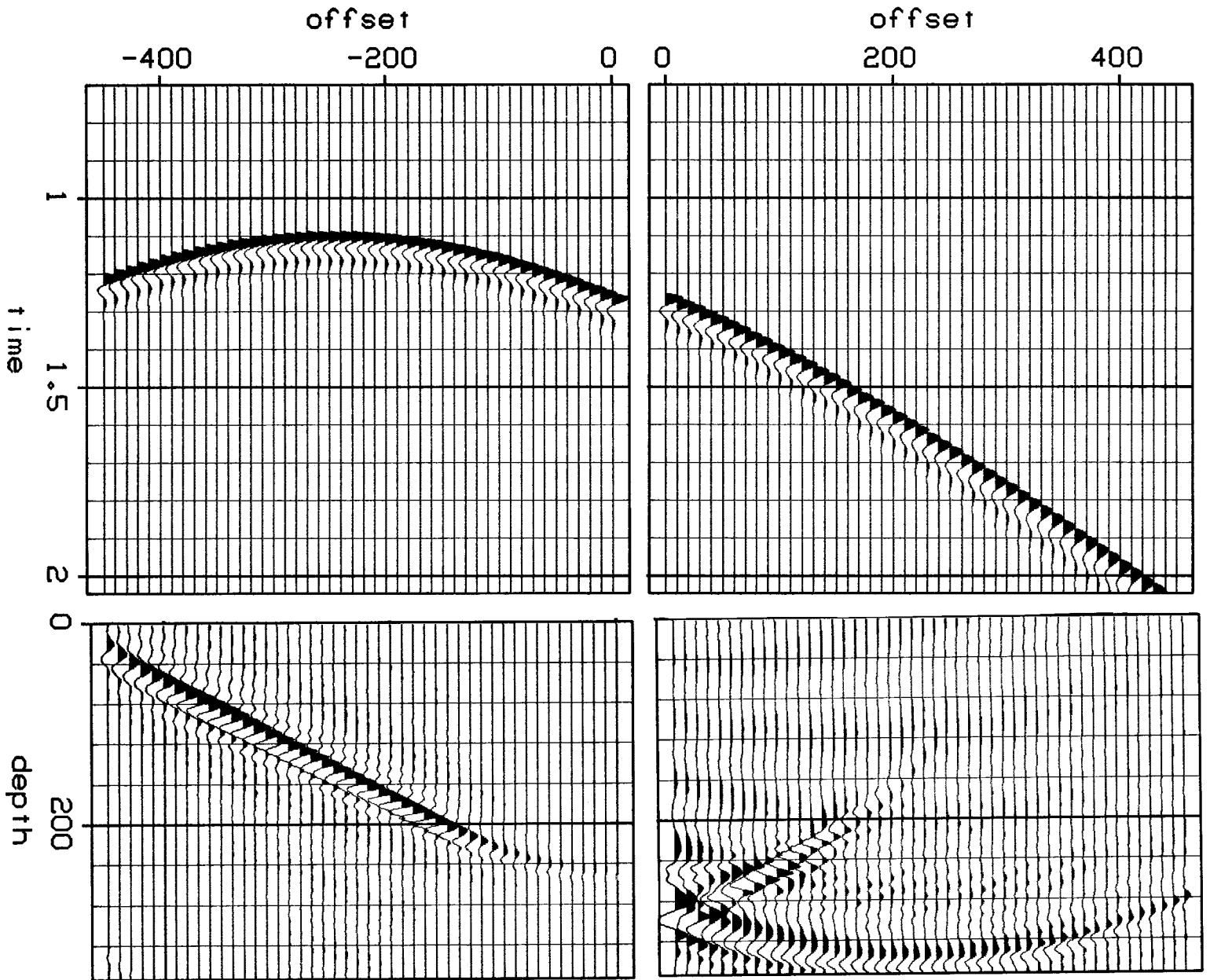


FIG. 2. Top: Left and right side portions of the profile in Figure 1. Bottom: Migrated portions of the profile. Note that The energy in the right side portion did not migrate to the correct place because the energy came from outside the cable. What is seen here is noise at a high gain.

CRG's have curved events for depths at which an incorrect velocity was used, while those obtained by use of the correct velocity have horizontal events (the first reflector in this case). The stacks of these migrated gathers appear in Figure 8. Note the lift that occurs at the right-hand side of the model where the migration velocity is too low.

There is a difference between the results of using Kjartansson's method and those using the hybrid method. Figure 9 shows a primary-only synthetic profile for a constant-velocity earth ($v=1000$ m/sec) with three reflectors at 200, 400, and 600 m. Figure 10 shows the results of migrating the profile with first our method and then Kjartansson's method, using each time the correct velocity and a low (600 m/sec) velocity. We know that, when the correct velocity is used, the extent of the image should be one-half of the cable's length, but the lower panel shows a smaller extent. The difference is more pronounced between the results of the low velocity. When we later use equation (3), we traverse a trajectory in the (x, z) plane to calculate the curvature of the event. This short extent makes it hard to distinguish between two close trajectories. We therefore see a tradeoff between these two methods. The hybrid method gives a long extent of the image but is slow, while the full extrapolation method is faster but gives a short extent.

Practical considerations

One of the parameters that need to be known is the frequency range that should be used to obtain a good image. This question is important because the more frequencies we have to use, the more costly using the algorithm becomes. Knowing the approximate spectrum of the data will help us determine its most significant range.

The depth steps were discussed in Paper I. We use a stripping method in which we disregard everything above an interface and concentrate on the events immediately below it. Our iteration of the velocity function will then be concerned only with that strip of the medium we are considering. We should bear in mind that this algorithm takes into account only those events that carry reflection information.

UPDATING THE VELOCITY

The underlying principle of this paper is

Use of only the correct velocity will make images from all offsets for a given point at the surface, form a horizontal line.

We can migrate the data with several trial velocities and then see what velocity function best satisfies this principle. However, it would be more economical to migrate once and then try to determine the amount of error in the velocity used in this first attempt.

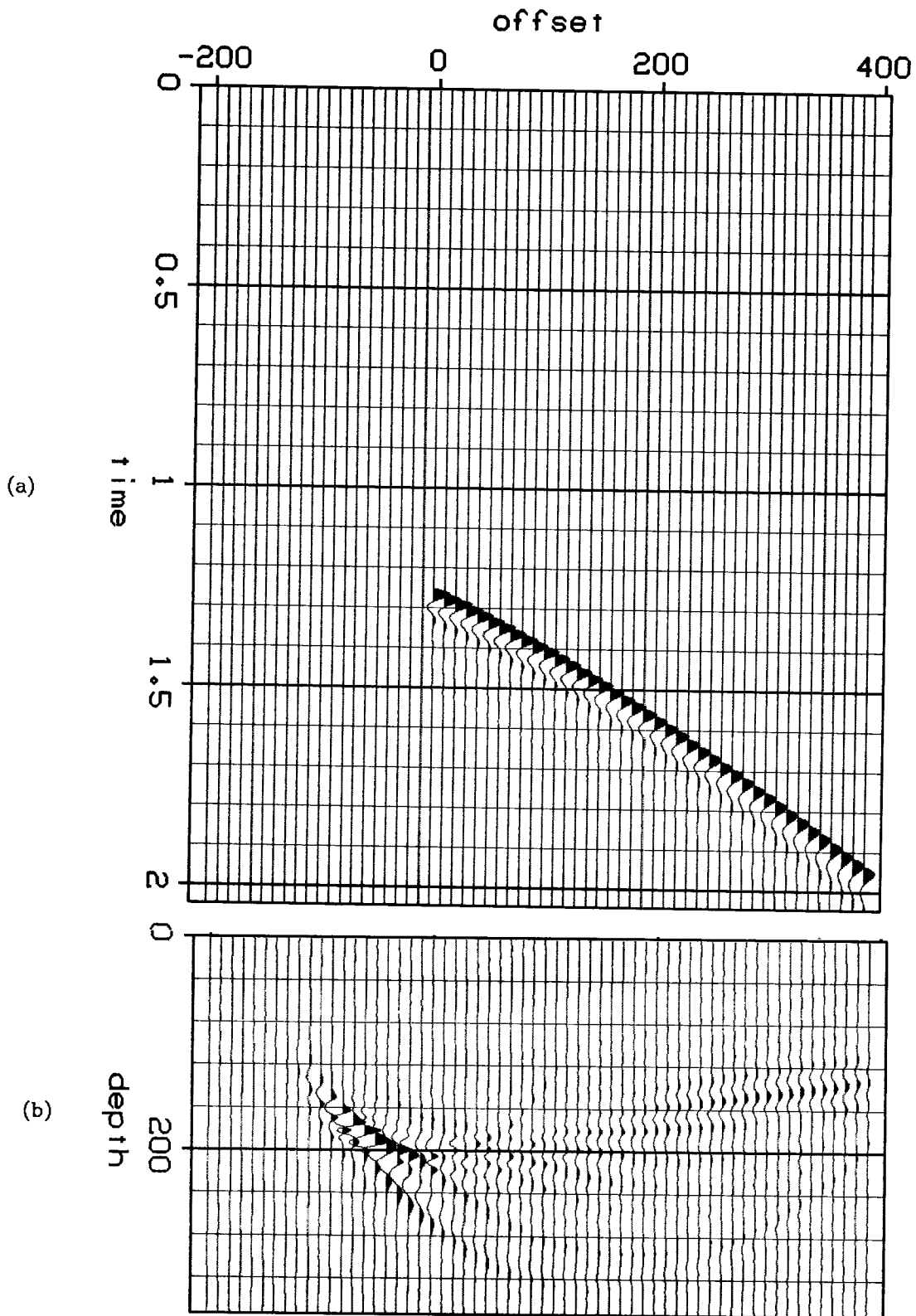


FIG. 3. (a) Right side portion of the profile in Figure 2 padded with zeros at the left. (b) The result of migrating the padded profile in (a). Compare (b) to Figure 2 (bottom right).

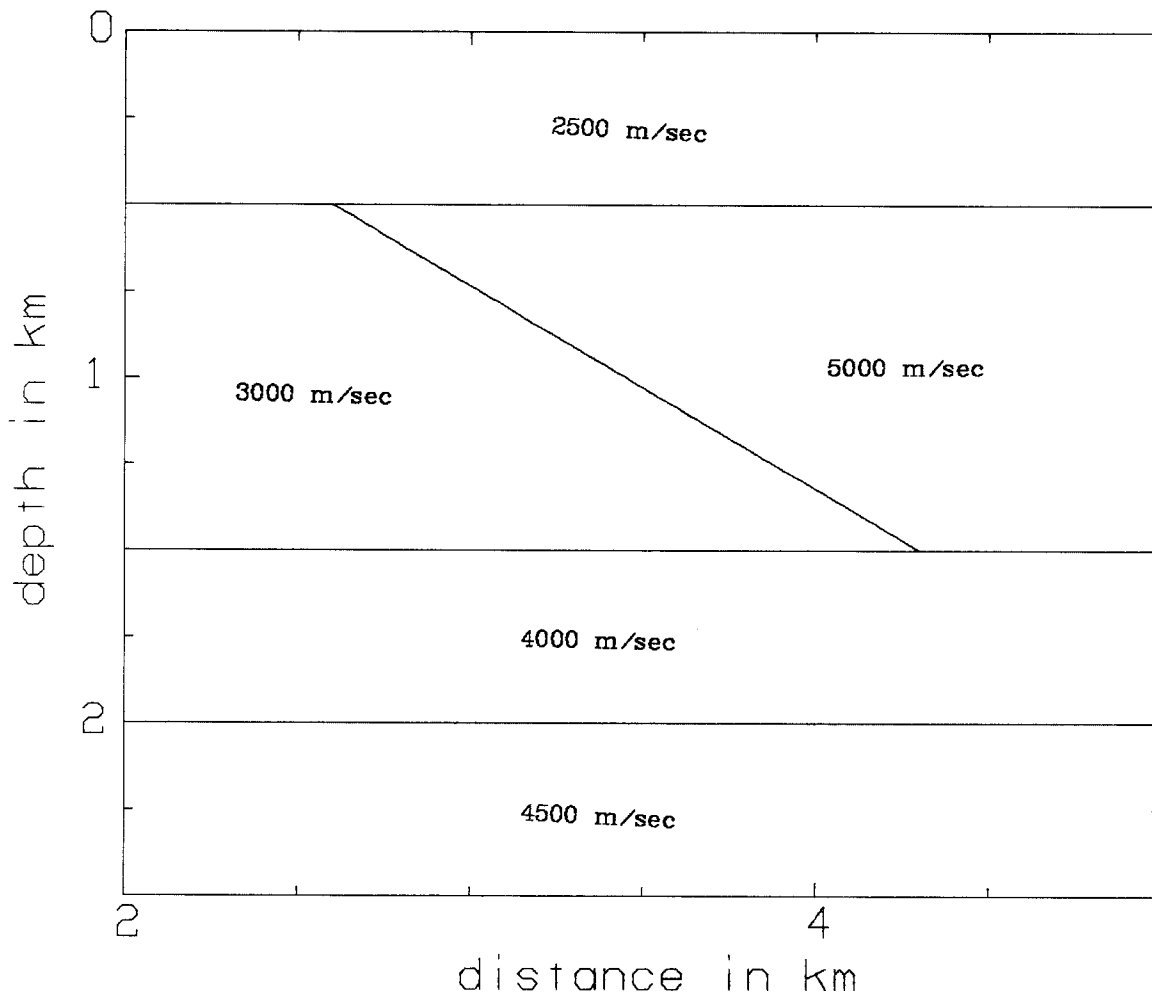


FIG. 4. A model having a strong lateral velocity variation plotted with the correct aspect ratio.

If we can make even an approximate estimate of the error, then we can migrate again with a more accurate velocity. We might also have to do one or more migrations to reach the best possible image.

We therefore hope to establish a way of quantifying the error in velocity. We will find this by looking at the kinematics of the problem. Our method consists of downward continuing the receiver at point x in Figure 11 to the depth z and then shifting by an amount equal to the travel time along sz . At point z we have the image that came from receiver g , the position of which should agree with that shown by a ray-tracing argument.

We will first discuss the application of this method to a horizontal reflector. Let the true depth be z , the true velocity be v , and the recorded travel time t , and let the incorrect depth be z_{wr} corresponding to the incorrect velocity v_{wr} . If we let the half offset be x ,

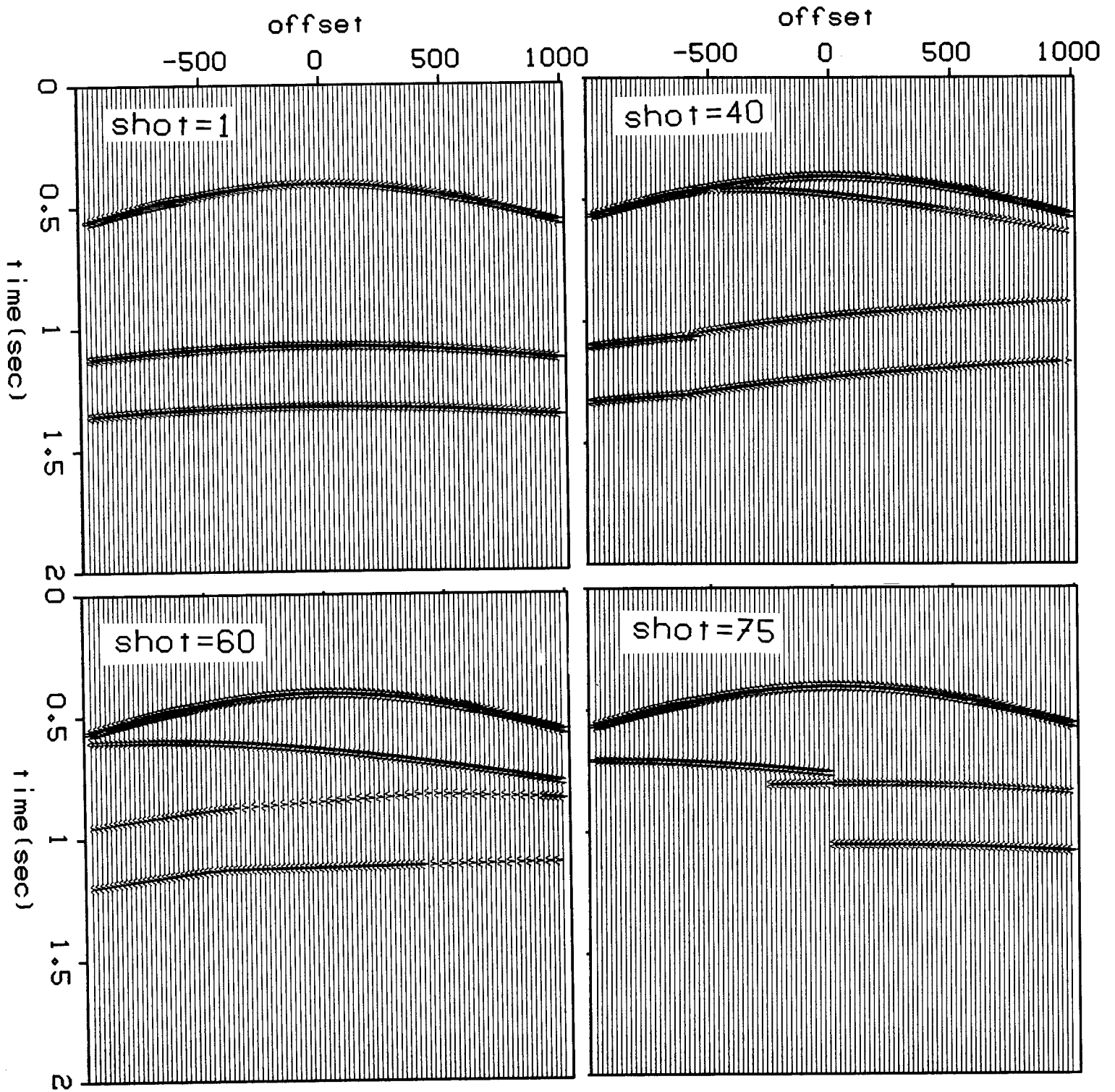


FIG. 5. Four primary-only synthetic profiles obtained from the model in Figure 4.

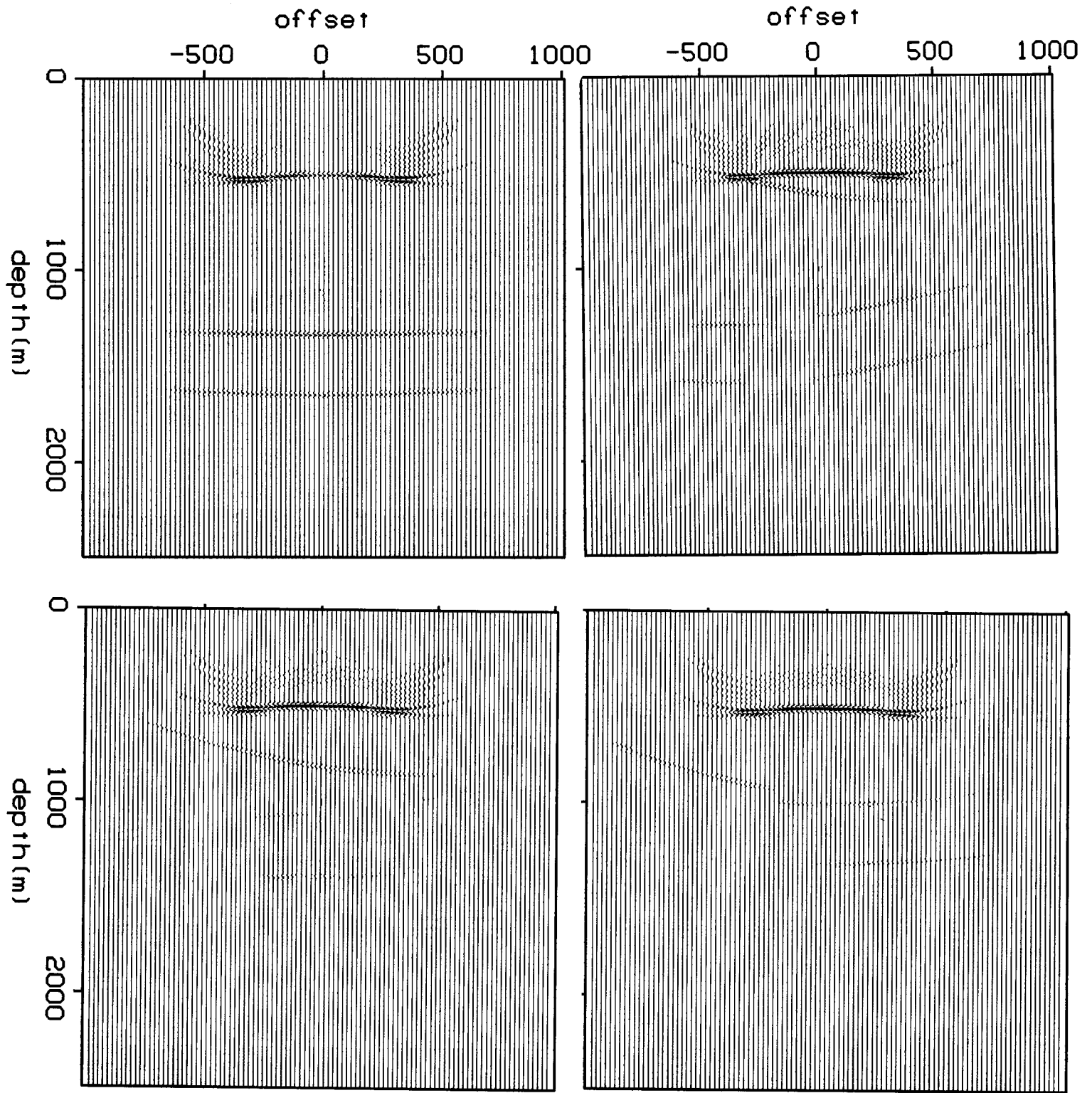


FIG. 6. The result of migrating the profiles in Figure 5 with a constant velocity of 2500 m/sec, which is the velocity of the upper layer. So the migration up to 500 m is correct.

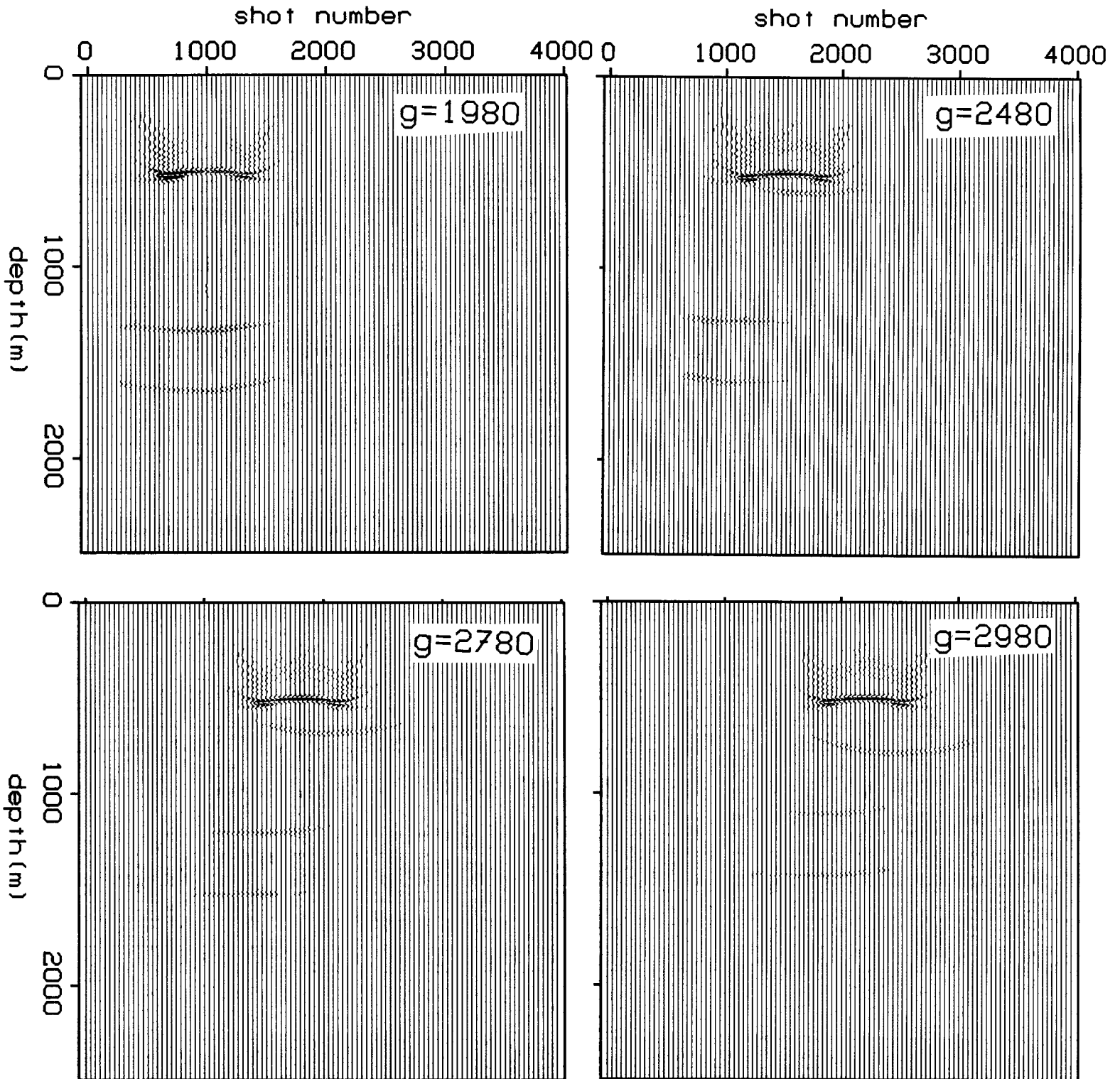


FIG. 7. CRG's obtained from the migrated profiles, some of which are shown in Figure 6.

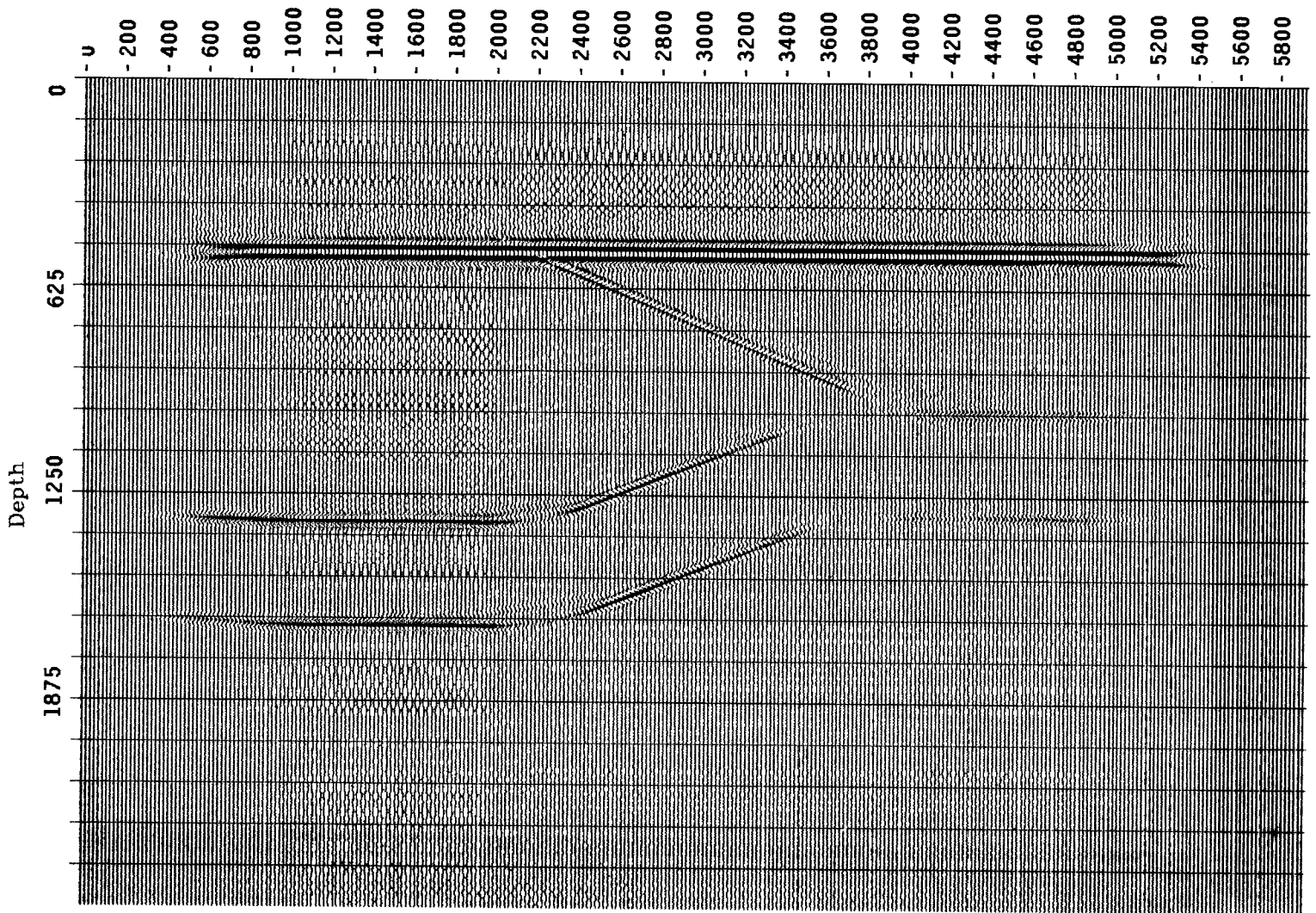


FIG. 8. The stack of the migrated profiles, using a constant velocity of 2500 m/sec.

then the travel time is given by

$$t = \frac{2\sqrt{x^2 + z^2}}{v} \quad , \quad (2a)$$

and for the incorrect velocity,

$$t = \frac{2\sqrt{x^2 + z_{wr}^2}}{v_{wr}} \quad , \quad (2b)$$

which gives

$$z_{wr}^2 = \frac{t^2 v_{wr}^2}{4} - x^2 \quad .$$

Substituting from (2a) for t we obtain

$$z_{wr} = \sqrt{\gamma^2(x^2 + z^2) - x^2} \quad , \quad (3)$$

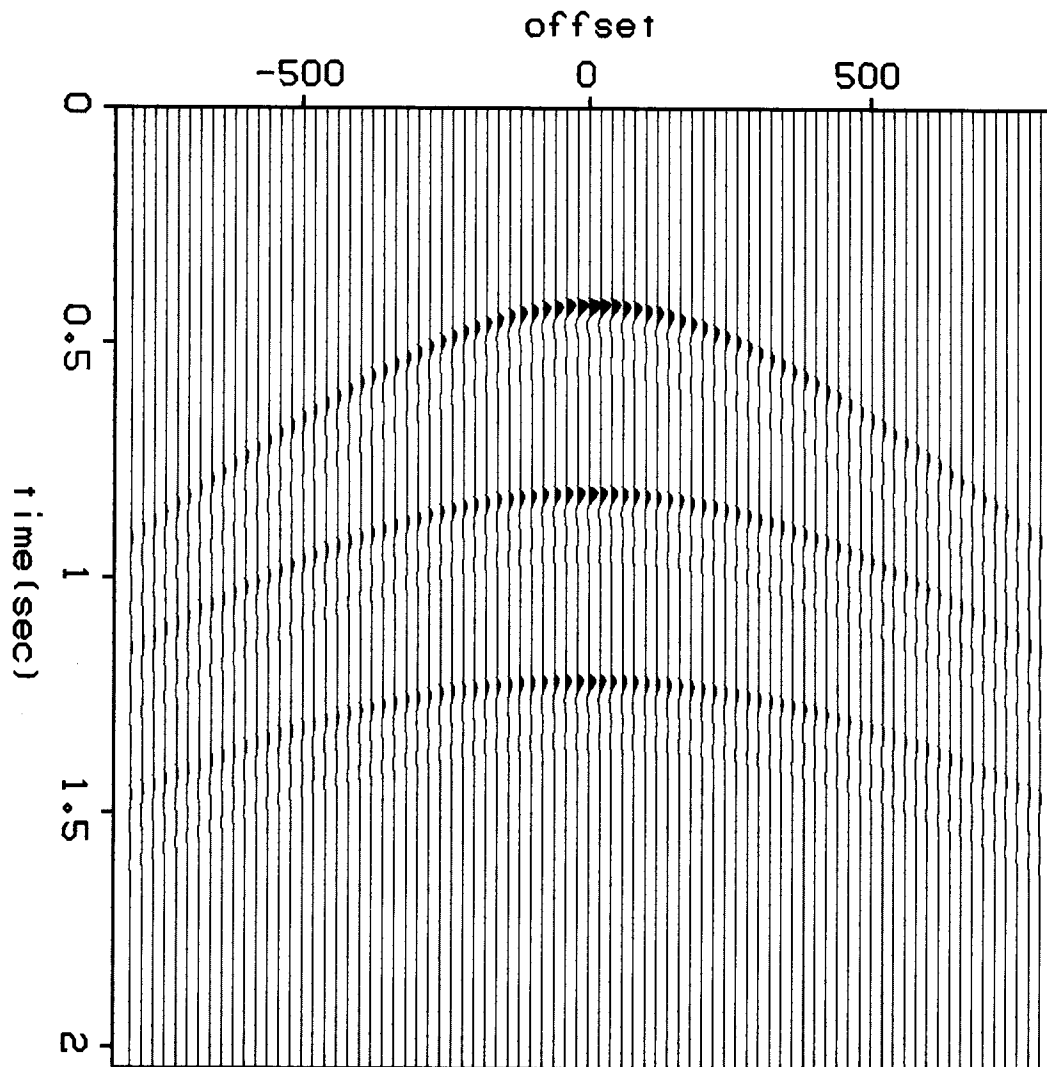


FIG. 9. A synthetic profile for a model having three reflectors at 200, 400, and 600 m and $v=1000$ m/sec.

where $\gamma = v_{wr}/v$.

Equation (3) is illustrated in Figure 12. Trajectories at two depths are shown to demonstrate that the usual deterioration of resolution with depth is present. Putting $\gamma = 1$ in equation (3) or looking at the plots verifies the principle described above. It is important to notice that this principle is true regardless of structure. This is due to the simple fact that when we study the image of the earth under a particular point at the surface, the image should be independent (in location) of the offset. Using an incorrect velocity produces two effects, a bulk shift and a curvature. The bulk shift comes from the relation $z_{wr} = \gamma z$ for $x = 0$. Because we do not know z , the actual depth, we can

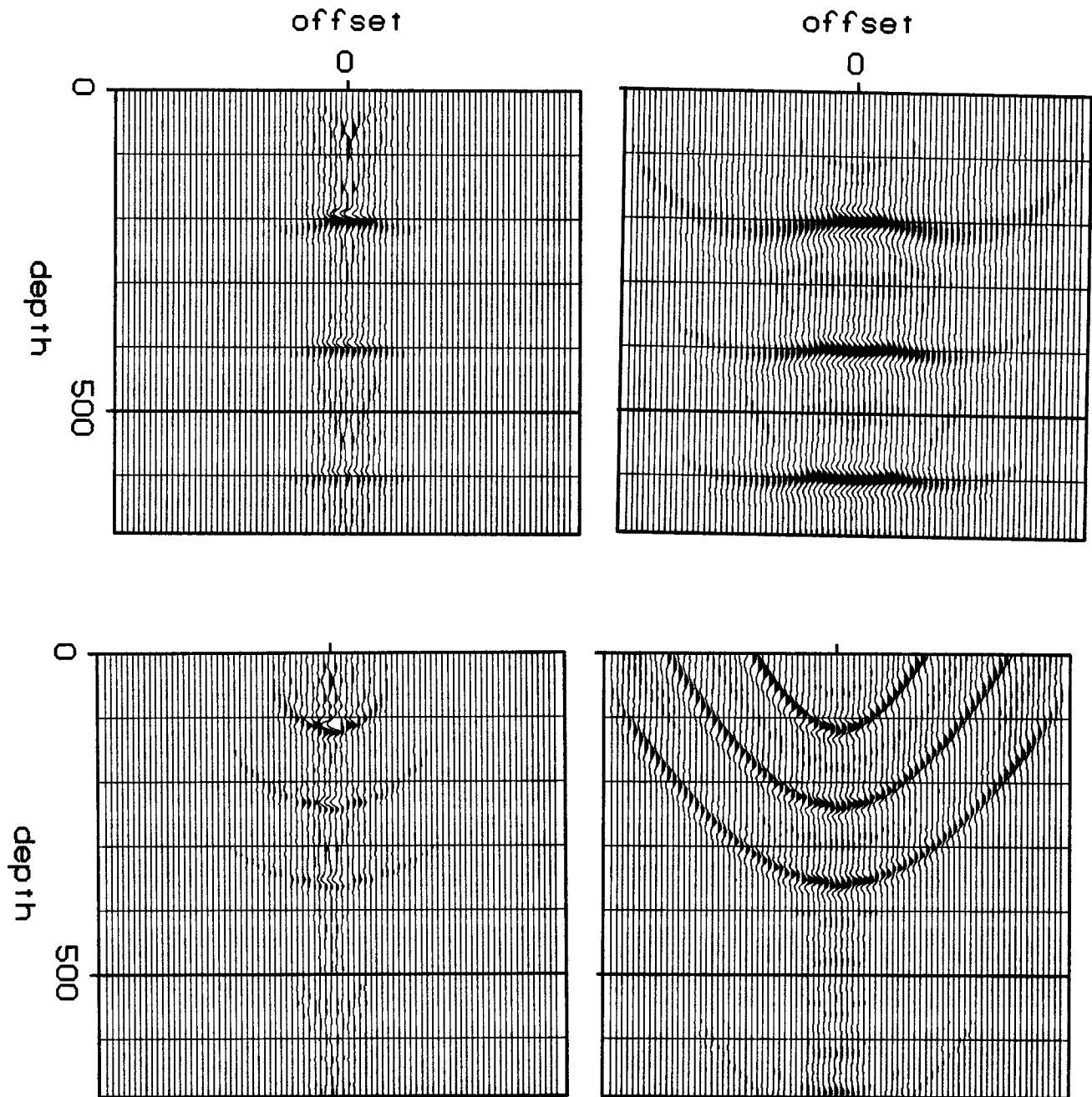


FIG. 10. The result of migrating the profile in Figure 9. Top: using a correct velocity (1000 m/sec). Bottom : using a low velocity (600 m/sec). The figures on the left are obtained by using Kjartansson's routine, and the ones on the right are obtained by using the hybrid method.

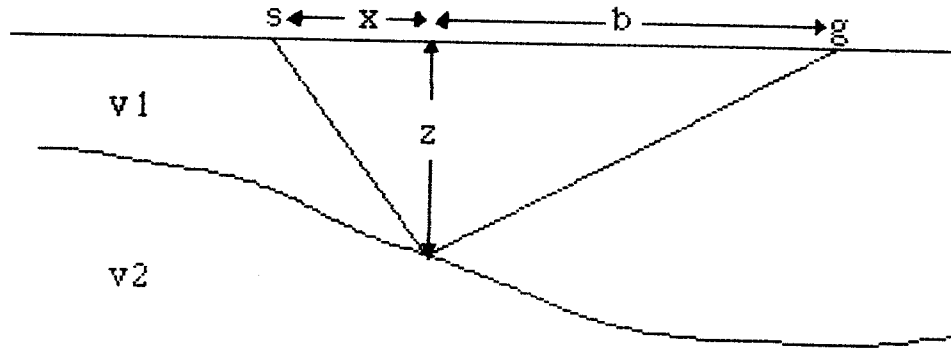


FIG. 11. The path along which the ray travels.

not use this bulk shift to detect the error in velocity. (With $x = 0$, the equation is the same as equation (9) of Yilmaz and Chambers (1984), which they used in their method of velocity analysis.) However, the curvature contains information that will help us correct our velocity model. Using an incorrect velocity causes the image to be offset-dependent. A low velocity causes smiles and a high velocity causes frowns. Thus in our second pass of migration we correct our velocity function according to the curvature of the previous result.

It is desired to derive an equation that is similar to equation (3) but is applicable to general reflector geometry. In the appendix we derive this equation, which is *structure dependent*.

$$z_{wr}^2 = \frac{\gamma^2}{4} f - \frac{x^2 + b^2}{2} + \frac{(x^2 - b^2)^2}{4\gamma^2 f} \quad , \quad (4)$$

where

$$f = x^2 + 2z^2 + b^2 + 2\sqrt{b^2 x^2 + b^2 z^2 + x^2 z^2 + z^4} \quad ,$$

and x , a , and b are as in Figure 11.

It is easily seen that equation (4) reduces to equation (3) if $x = b$ (a horizontal reflector), and that $z_{wr} = z$ if $\gamma = 1$. We can further simplify this equation by noticing that the last term is negligible in comparison to the other two (actually, it vanishes for a horizontal reflector because $a = b$ in this case), and thus reach

$$z_{wr}^2 = \frac{\gamma^2}{4} f - \frac{x^2 + b^2}{2}$$

In deriving equation (4), we did not make assumptions on the structure of the subsurface. We did, however, assume that s , g , and z are located in a homogeneous layer,

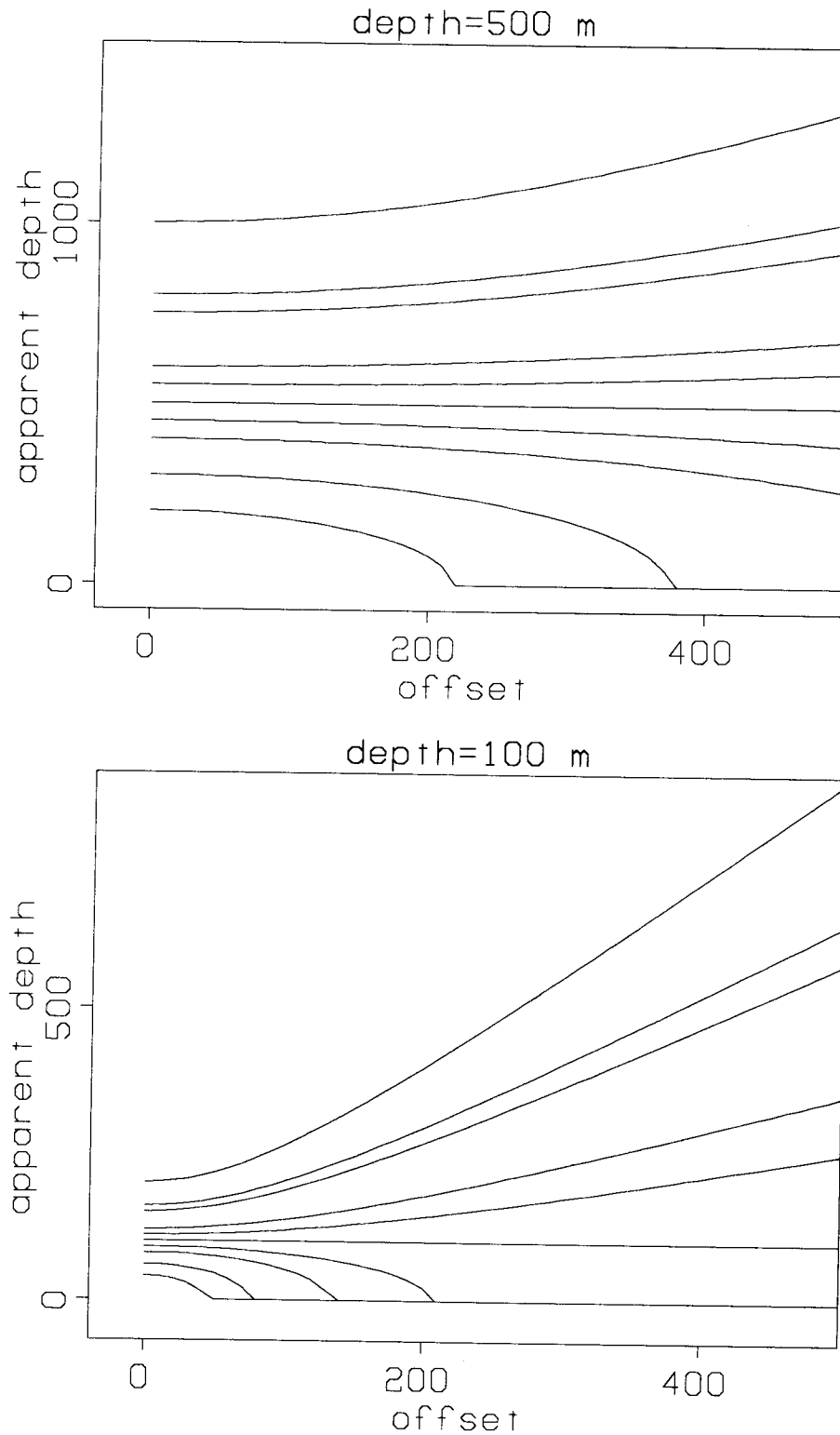


FIG. 12. Trajectories showing the apparent depth as a function of offset for several γ values. Top: true depth=100 m. Bottom: true depth=1000 m. γ values, from the bottom, are .4, .6, .8, .9, 1, 1.1, 1.2, 1.5, 1.8, 2.

that is, there is no velocity variation between s , g , and z . The structure dependency of equation (4) makes it hard to calculate the residual velocity from the curvature of the events, because one needs the partition of the offset, not the offset alone, in order to search for the possible path of the ray. Nevertheless, it should be noticed that, according to the principle stated above, the horizontal alignment of images in migrated common receiver gathers (CRG's) will take place only when the velocity is correct; this fact should be made use of. (By a CRG we mean the traces that have the same g -coordinate as those shown in Figure 13. It does NOT mean traces that were recorded by the same receiver.)

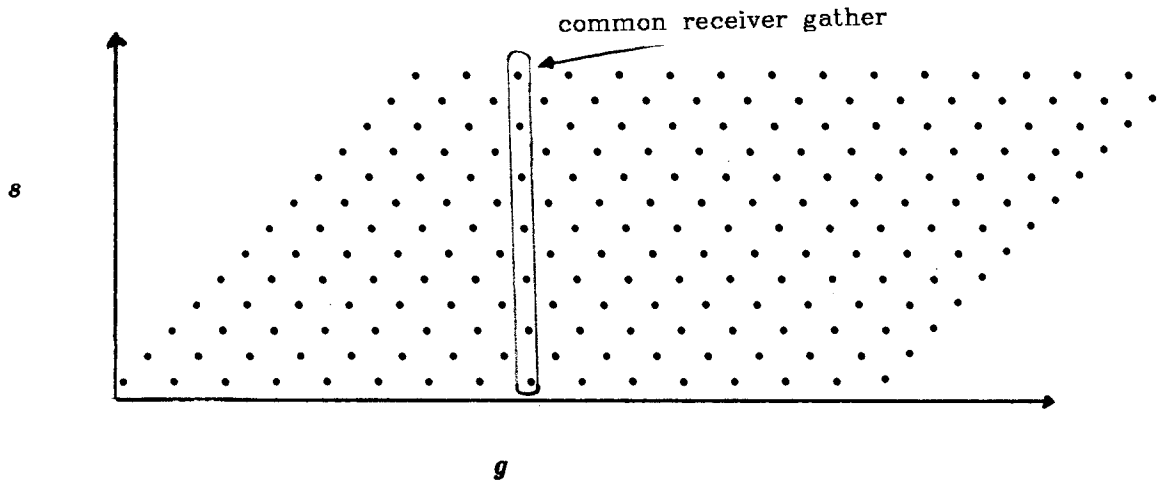


FIG. 13. A common receiver gather.

Unlike equation (3), the trajectory of equation (4) is asymmetric. It is still not clear whether this asymmetry is helpful in updating the velocity. It is clear, however, that it is structure dependent.

The user of this method must be aware of the fact that not all migrated CRG's will give correct information. Because of edge effects, those receivers near the end of the illuminated area, will not be aligned even when the correct velocity is used.

TWO ILLUSTRATIVE EXAMPLES

We will first give an example showing the qualitative difference between the migrated CRG's obtained with the correct and with the incorrect velocity. Figure 1 shows the model used in this example. In order to perform velocity analysis, we need to record several profiles. Even when velocity analysis is not the target, using several profiles provides a means for signal-to-noise improvement.

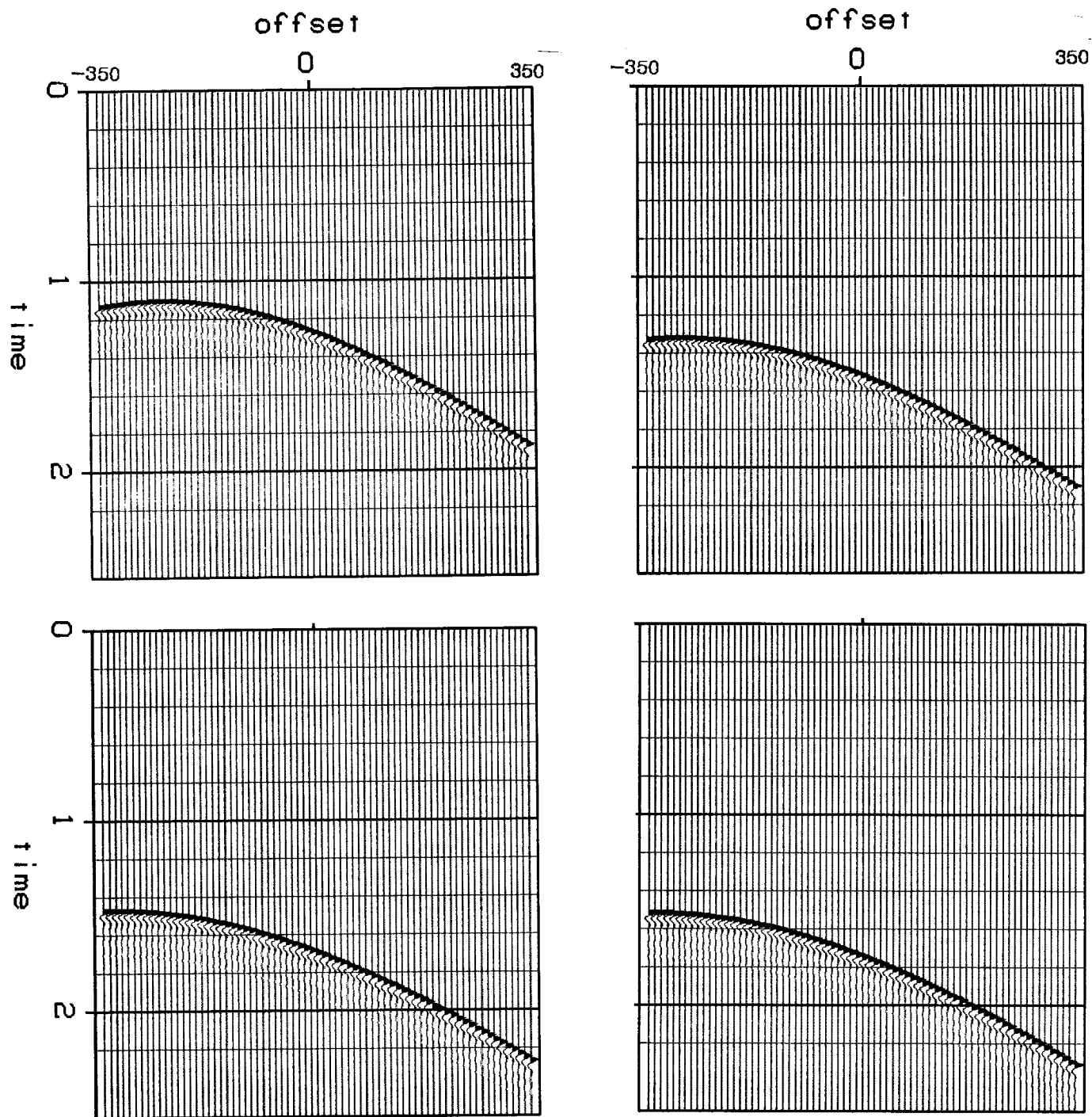


FIG. 14. Four primary-only synthetic profiles from the model in Figure 1. Their numbers clockwise from top left are 1, 11, 17, 20. The parameters are: $nt=1024$, $ng=71$, $nshot=20$, $dt=4$ msec, $dg=10$ m, and $dshot=10$ m.

Figure 14 shows four of twenty profiles recorded. Figures 15 and 16 show the results of migrating the profiles with the correct and with the incorrect velocity, respectively. Note that structure is manifested in these profiles one way or another. The result of stacking the migrated profiles is shown in Figure 17. Notice that if we do not know the velocity, the result of migration can be misinterpreted. We presume that we do not know at this stage if the velocity is correct and the result is the true image, or if the velocity is incorrect and the result is not the true image.

The next step is to sort the migrated profiles to obtain CRG's, some of which are shown in Figure 18. These CRG's should reflect no structure when the velocity is correct, as stressed before. For this example, we have not attempted to quantify the error in the velocity, because we can not easily determine this error for a non-horizontal reflector. We can, however, infer qualitatively that the velocity used in the second case is low, because the migrated CRG's had events that curved upward (smiles), while the velocity in the first case is correct because events were horizontal.

Now, we will attempt to quantify this error for a horizontal reflector. For this purpose, we will use the earlier results of Figure 10.

Because the reflectors are horizontal, then common receiver gathers and common shot gathers are identical. We can therefore test equation (3) on the gathers in Figure 10, and determine the trajectory with the maximum energy. The result of this calculation is shown in

Figure 19, where we used a suite of velocities in our search and contoured the result. We see that the maximum coherence will be reached only by using the correct velocity ($\gamma = 1$). Of course, these coherences occur at the correct depths (besides a couple of maxima that indicate the use of high velocities, but whose amplitude is low). When using the incorrect velocity, the maximum coherence occurs at $\gamma = .6$, also besides more maxima. However, in this case, the maxima are not of very small amplitude to be ignored but they fall very close to $\gamma = .6$. (the one we used). Our inability to exactly quantify the error in velocity is a result of using an approximate equation (the 45° equation) for the downward continuation. However, it is obvious that we will be much closer to the correct velocity in the next iteration than we were in the first.

CONCLUSIONS

We have demonstrated that velocity analysis based on the wave equation is possible. We have also shown that migrated CRG's furnish a suitable domain for such analysis. The principle we used was that the alignment of images in these gathers will take place

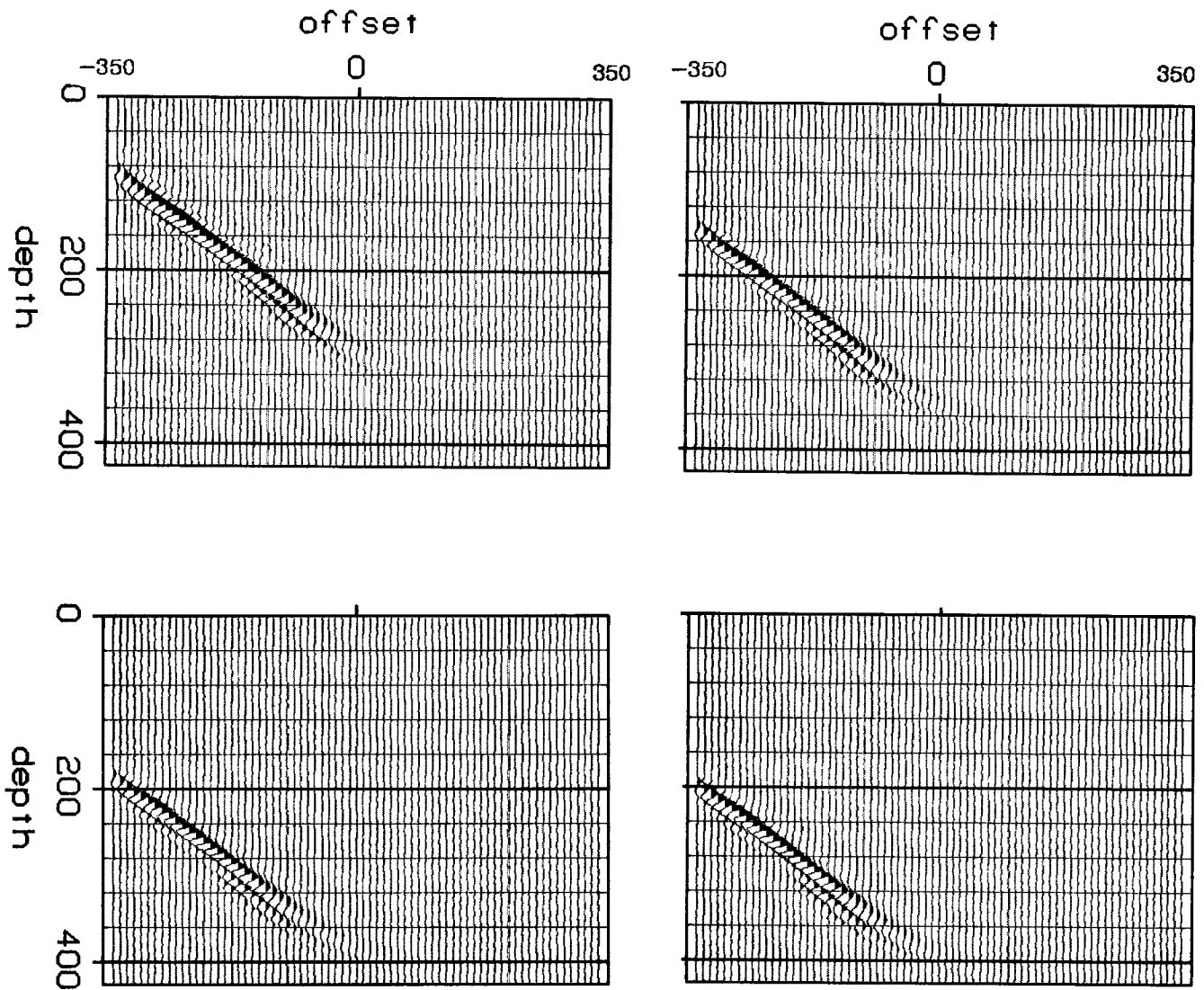


FIG. 15. The result of migrating the profiles in Figure 14 with the correct velocity (400 m/sec), $dz=6$ m.

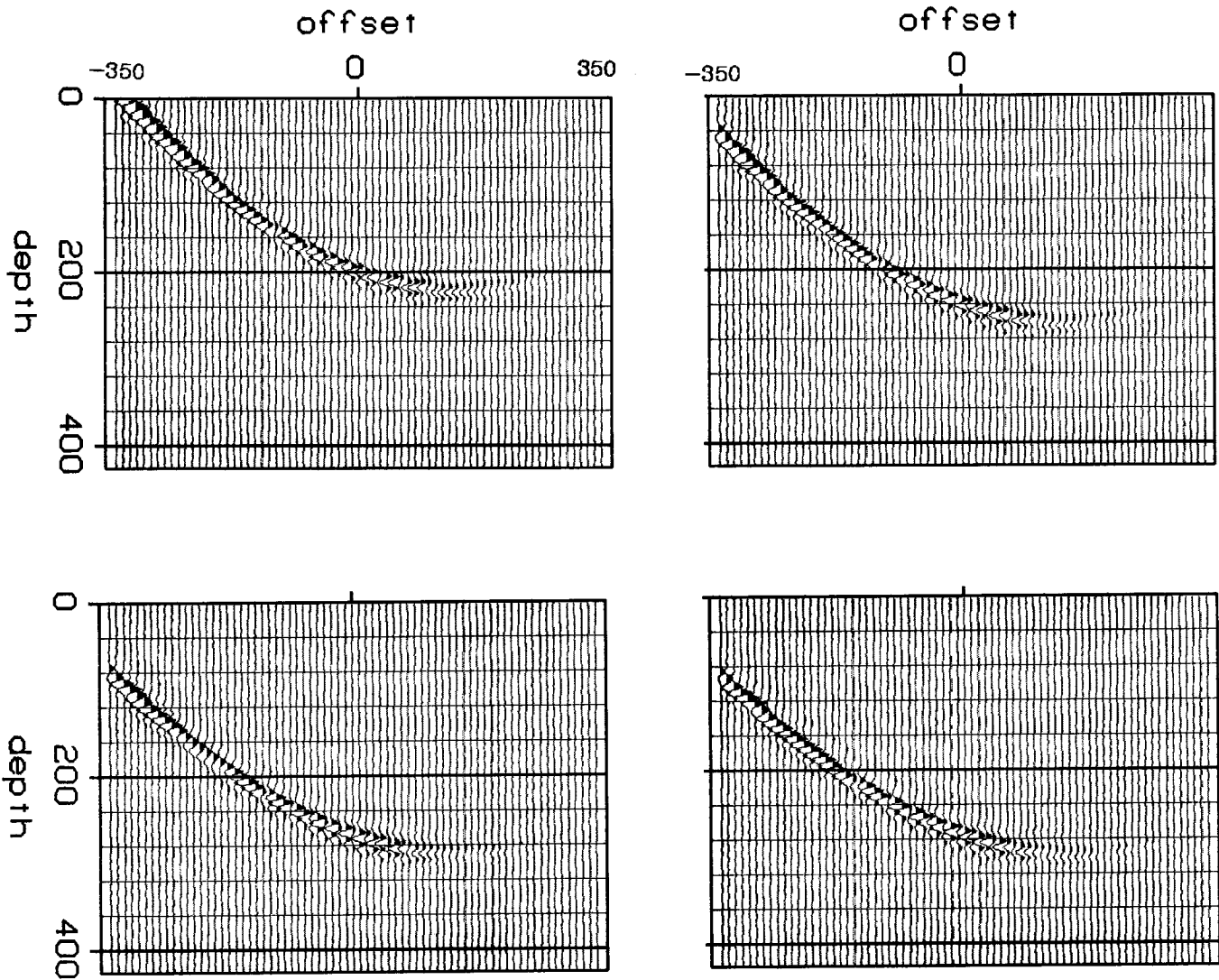


FIG. 16. The result of migrating the profiles in Figure 14 with the wrong velocity, (300 m/sec) $dz=6$ m.

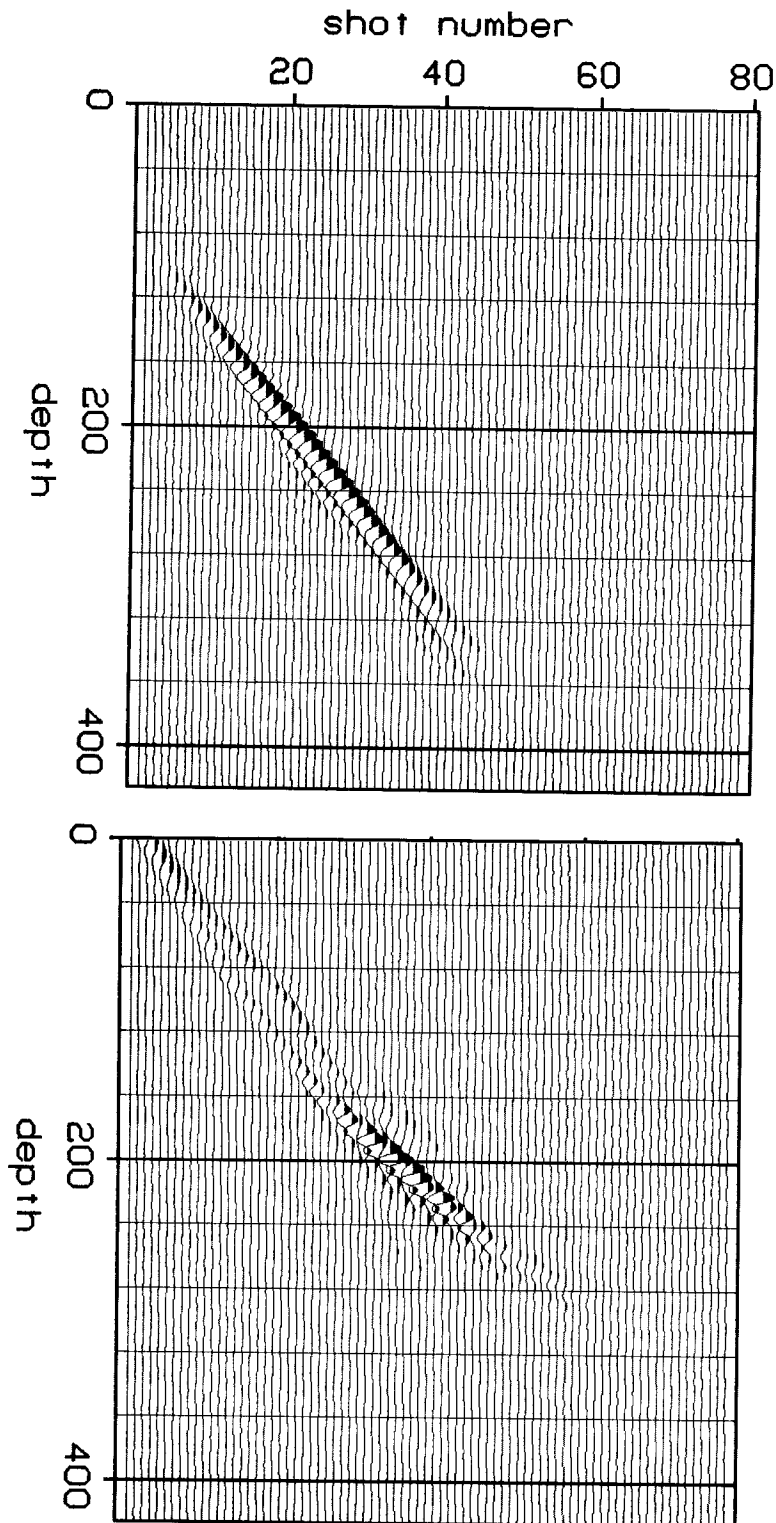


FIG. 17. The stacks of the migrated profiles, using the correct velocity, 400 m/sec, (top) and the low velocity, 300 m/sec, (bottom).

only when we are using the correct velocity; this fact is independent of the structure. The residual velocity is easily known from the curvature only for horizontal reflectors. The whole procedure is summarized in Figure 20.

The main shortcoming of the method that we used, as of other velocity analysis methods, is its disregard of non-structural properties. For example, we cannot use this method if a velocity gradient exists within a layer. On the other hand, at one stage of this method, we look at common receiver gathers, which help us to study the angular dependence of reflectivity.

Prestack migration can be used to study converted waves, too. For example, to study a converted S-wave from a reflector when we know the P-wave for the medium, we can iterate the S-wave velocity while downward continuing the receivers to that reflector, until we obtain alignment for images in the migrated CRG's. That alignment indicates that we used the correct S-wave velocity.

An argument was made in this paper of the advantage of wide-angle split-spread profiles. Such recording should be done, whenever possible, for both land and offshore prospects. Of course, the reader will wonder how split-spread recording can be done offshore. We will not address this question here.

ACKNOWLEDGEMENTS

We thank Ivan Psencik for helping us to use the raytracing package and for modifying it to suit our purposes. We also thank Einar Kjartansson for many useful discussions and for providing his prestack migration program that was used to generate Figures 6, 7, and 8.

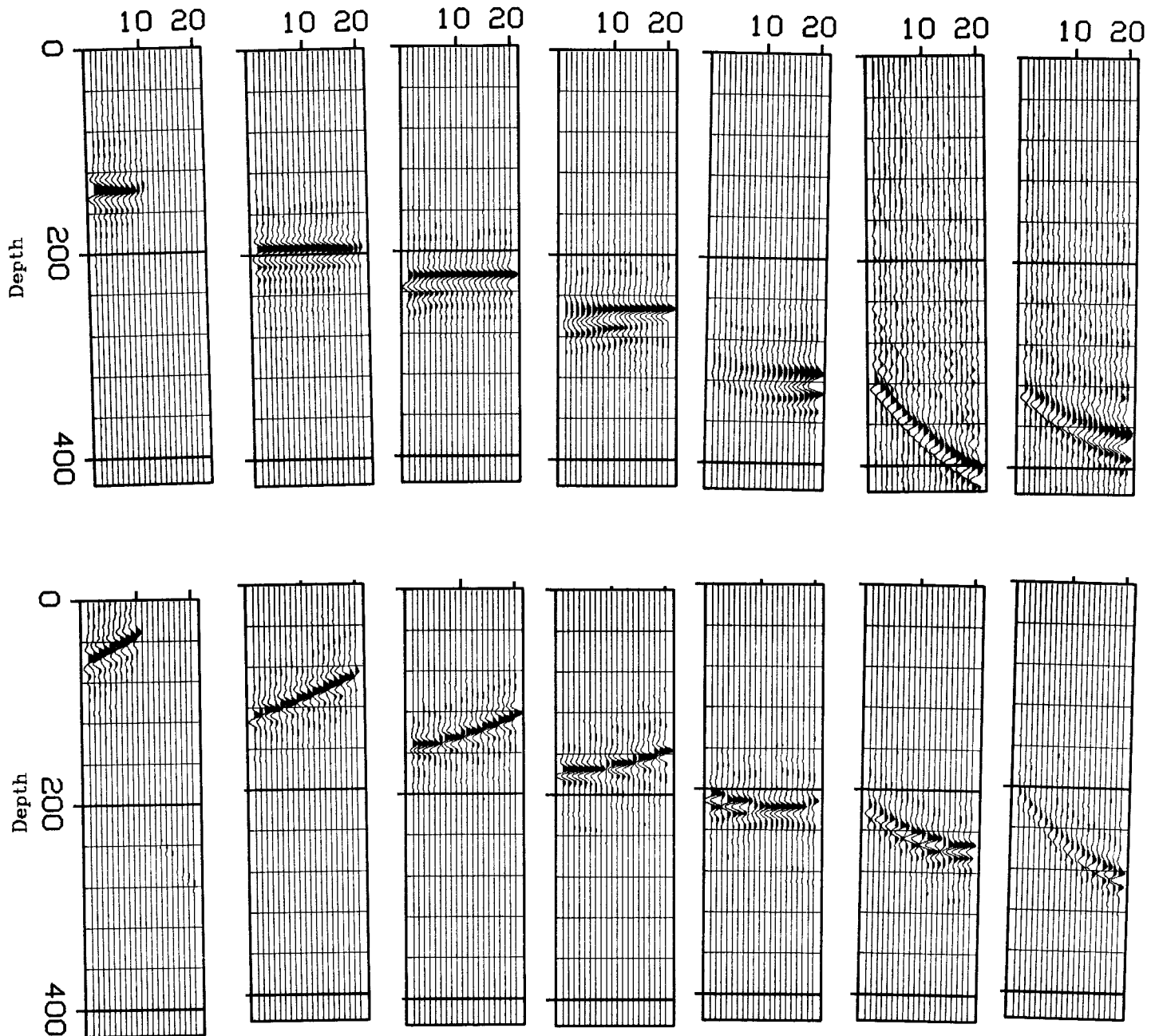


FIG. 18. Common receiver gathers from the migrated profiles in Figures 15 and 16. The top panel is from Figure 15 (using the correct velocity) and the bottom panel is from Figure 16 (using the wrong velocity). The locations of these gathers correspond to receivers number 1,11,17,21,41,51,61 in profile number one. Note that the last two gathers are displayed at high gain.

REFERENCES

- Al-Yahya, K., and Muir, F., 1984, Velocity analysis using prestack migration, SEP-38, p. 105-113.
- Doherty, S. M., and Clærbout, J.F., 1974, Velocity analysis based on the wave equation, SEP-1, p. 160-178.
- Jacobs, A., 1982, The prestack migration of profiles, Ph.D. thesis, Stanford University.
- Kjartansson, E., 1983, Processing of crustal reflection data in the presence of strong lateral velocity inhomogeneities: presented at the AGU 1983 fall meeting, San Francisco.
- Yilmaz, O., and Chambers, R. E., 1984, Migration velocity analysis by wave-field extrapolation, Geophysics, v. 49, p. 1664-1674.

APPENDIX

The travel time t between the source and receiver in Figure 4 is

$$t = \frac{\sqrt{x^2 + z^2}}{v} + \frac{\sqrt{b^2 + z^2}}{v} \quad , \quad (\text{A} - 1)$$

from which we obtain

$$t^2 v^2 = x^2 + z^2 + b^2 + z^2 + 2\sqrt{b^2 x^2 + b^2 z^2 + x^2 z^2 + z^4} \quad (\text{A} - 2)$$

To simplify the algebra we will write equation (A-2) as

$$t^2 v^2 = f \quad (\text{A} - 3)$$

An equation similar to (A-2) can be obtained for the incorrect velocity, v_{wr}

$$t^2 v_{wr}^2 = x^2 + z_{wr}^2 + b^2 + z_{wr}^2 + 2\sqrt{b^2 x^2 + b^2 z_{wr}^2 + x^2 z_{wr}^2 + z_{wr}^4}$$

Squaring both sides,

$$\begin{aligned} t^4 v_{wr}^4 + x^4 + 4z_{wr}^4 + b^4 - 2t^2 v_{wr}^2 x^2 - 4t^2 v_{wr}^2 z_{wr}^2 - 2t^2 v_{wr}^2 b^2 + 4x^2 z_{wr}^2 + 2x^2 b^2 + 4z_{wr}^2 b^2 \\ = 4b^2 x^2 + 4b^2 z_{wr}^2 + 4x^2 z_{wr}^2 + 4z_{wr}^4 \quad , \end{aligned}$$

from which we obtain

$$z_{wr}^2 = \frac{t^4 v_{wr}^4 + x^4 + b^4 - 2t^2 v_{wr}^2 x^2 - 2t^2 v_{wr}^2 b^2 - 2b^2 x^2}{4t^2 v_{wr}^2}$$

Substituting for t from equation (A-3),

$$\begin{aligned} \frac{\gamma^4 f^2 - 2\gamma^2 f(x^2 + b^2) + (x^2 - b^2)^2}{4\gamma^2 f} \\ \gamma = \frac{v_{wr}}{v} \end{aligned}$$

from which equation (3) was obtained.

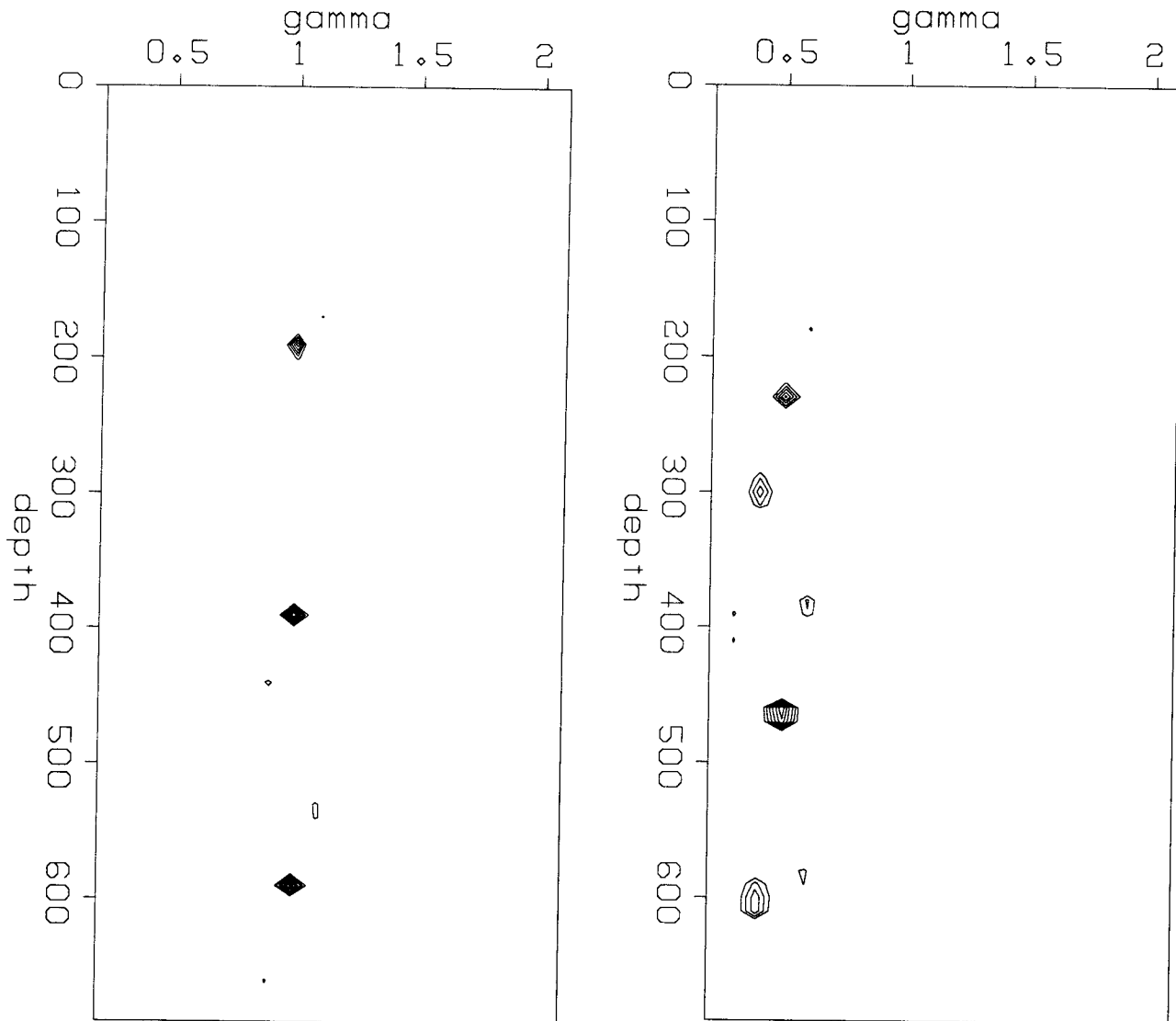


FIG. 19. The results of calculating the error in velocity in the profiles of Figure 10. Note that $\gamma = v_{wr}/v$. The left figure comes from the top part of Figure 10 in which the migration velocity was correct, while the right figure comes from the bottom part of Figure 10 in which the migration velocity was low.

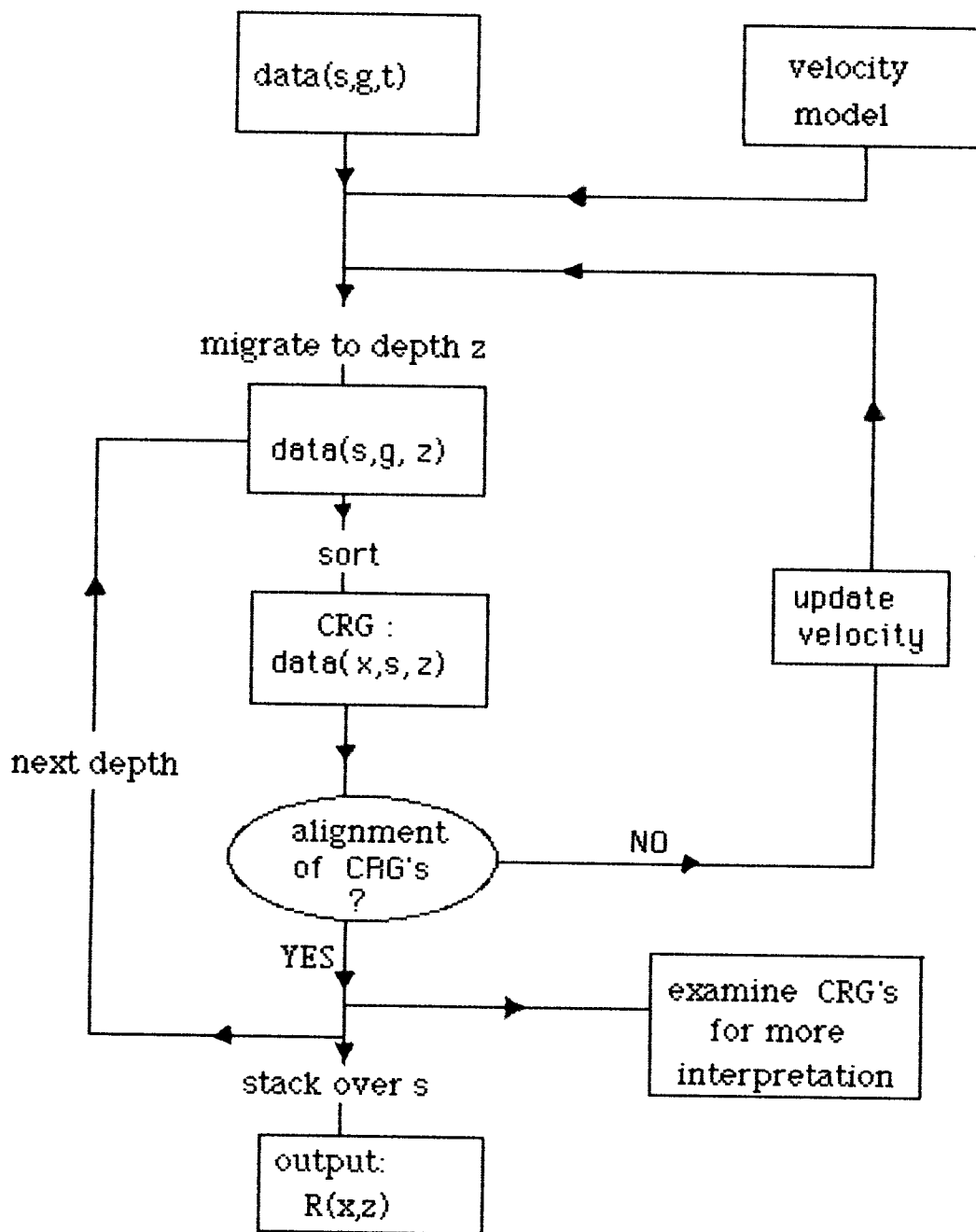


FIG. 20. A flow chart showing a summary of the procedure outlined in this paper.



Along the intruder-detection zone
(from the Soviet book *Guardians of the Border*)